

## 9.5 Gyr of evolution of galaxies in clusters

Irene Pintos-Castro<sup>1,2</sup>, Miguel Sánchez-Portal<sup>3,2</sup>, and Bruno Altieri<sup>3</sup>

<sup>1</sup> Centro de Astrobiología, INTA/CSIC, Madrid, Spain

<sup>2</sup> ISDEF, Madrid, Spain

<sup>3</sup> European Space Astronomy Centre (ESAC), Villanueva de la Canada, Madrid, Spain

### Abstract

“A database of 9.5 Gyr of evolution of galaxies in cluster” is an ESA EXPRO project to build a database of nine clusters at  $0.4 \leq z \leq 1.6$  observed by *Herschel*, in order to characterise their obscured star formation properties. For these clusters we have elaborated multi-wavelength catalogues of cluster member candidates (including the photometric redshift determination based on SED-fitting and Monte Carlo simulations), and built a comprehensive database containing a large set of physical properties (e.g. stellar mass, SFR, projected local density), an AGN discrimination, and a morphological classification for those clusters at  $z \leq 1$ . With the full dataset in hand we are addressing two main questions: is there a reversal of the SFR-density relation in this sample? and, what is the relationship between the cluster mass and the total star formation rate? Regarding the last question we are extending the work of [16] with a cluster sample above  $z \sim 0.8$ . Furthermore, with the AGN discrimination based on IRAC colours, we are able to analyse the fraction of AGN so we will trace also the AGN-density relation [13] and the evolution of this population up to  $z \sim 1.6$ . In particular we are studying the fraction of AGN as a function of the local galaxy density at high redshift, and comparing it with the SFR-density relation, to study the possible environmental co-evolution of both populations [12].

### 1 Introduction

Since early '90s, the quantity of studies about the star formation rate density and the stellar mass assembly from  $z \approx 0$  to the alleged last reionisation epoch has grown geometrically. As a result, today it is quite clear that the star formation rate density has a peak around  $z \approx 2$  with an amplitude about 10 times that measured in the local universe, whereas the mean stellar mass decreases monotonically. Also, a trend in the number density of active galactic nuclei (AGN) appeared to be placed at  $z = 1.5\text{--}2$ . Yet very recently, the number of high redshift galaxies (beyond  $z = 7$ ) has increased dramatically, together with the studies

Table 1: List of clusters included in our “9.5 Gyr of evolution of galaxies in clusters”

Cluster name	z	Available data	No. Mem.	No. FIR emi.
ClG 0024+1654	0.395	H $\alpha$	-	-
RX J1257+4738	0.866	[OII],FIR	315	37
ClG J1226+3332	0.89	FIR	182	8
WARPS J1415.1+3612	1.03	FIR	385	12
RX J0848.9+4452 (Lynx E)	1.27	FIR	993	42
XMMU J2235.3-2557	1.393	FIR	123	8
CXO J141520.1+361027 <sup>a</sup>	~1.52	FIR	261	0
XDCP J0044.0-2033	1.58	FIR	38	4
XMM-LSS J02182-05102	1.62	FIR	615	68

<sup>a</sup>within the field of WARPS J1415

devoted to the role of environment in galaxy evolution. It was first suggested by [6] that galaxy morphology depends on the environment. However, only in the last years this dependence has been quantified and extended to other characteristics. The results so far show that although mass is certainly the main driving parameter, environmental density plays an important role not only in morphology, but in dynamics [1], SFR of low-mass galaxies [11], AGN activity [12], metallicity [19], just for mentioning only some works in this subject. Nevertheless, environmental effects are far to be fully understood yet. For example, it is puzzling that the impact of the environment on a galaxy seems to be independent of its stellar mass. This might indicate that the stripping of an extended gas reservoir predominantly occurs via tidal forces rather than ram-pressure. However, the impact of environment in low-mass galaxies have not been properly taken into account yet. On the other hand, the investigation of the properties of high-redshift galaxy clusters is becoming crucial for our understanding of the early evolution of the Universe, since the existence of virialised clusters with fully established early-type galaxy populations can subject the assumed Gaussianity of the primordial density field to a critical revision (a dramatic case is the mature cluster at  $z = 2.07$  discovered by [8]). The present project aims to complete the studies in this recently competitive field, investigating the evolution of the galaxy population in clusters at intermediate to high redshift, focusing in star formation rates, morphologies, and the debated role of AGN in the process. We take benefit from the FIR and MIR spectral ranges that uncover the obscured star formation and AGN activity by means of *Herschel* and *Spitzer* photometric data. In addition, we will provide the scientific community with a comprehensive database of galaxies in clusters ready to be exploited.

## 2 The database

The sample is formed by nine galaxy clusters observed via the *Herschel* Guaranteed Time programme (P.I. Altieri, which includes six clusters and six proto-clusters), the two first

targets of the GLACE survey [17], and one additional cluster that was detected within the field of one of the *Herschel* clusters. In Table 1 we show the complete list of clusters, along with their redshift and the star formation estimation approach (i.e. emission-line flux, from GLACE, and/or FIR from *Herschel* clusters).

## 2.1 The multi-wavelength catalogues

In order to define reliable samples of cluster members, the first step is to build a multi-wavelength UV/optical-to-NIR catalogue. Following [15], we cross-matched the optical catalogues with NIR, MIR(IRAC), and UV(GALEX) catalogues, using the nearest-neighbour technique following [7] and the [5] methodology. As general conditions we used a maximum error radii of 2'' from optical to NIR bands, of 3'' for the IRAC channels, and of 4'' for GALEX bands, and we kept in the initial catalogue all sources from each catalogue from the optical to the MIR<sup>1</sup>. Prior to the photometric redshift estimation we adapted these initial catalogues both to the format of the code to fit the SED and to an appropriate length (considering only objects with at least three optical bands, or even more depending on the size of the initial catalogue).

## 2.2 Determination of cluster membership

These adapted catalogues were used to estimate photometric redshifts by SED-fitting the stellar part of the spectrum with [2] templates using the *LePhare* code [9], and using Monte Carlo simulations we defined a set of criteria to determine the cluster membership.

The galaxies cluster membership was determined through Monte Carlo simulations: (i) we created 1000 mock catalogues by randomly varying every band flux within its error<sup>2</sup>; (ii) we fitted the SED with *LePhare*, see Sect. 2.2.1, obtaining both a photometric redshift distribution (with 1000 values) for each source and 1000 photometric redshift distributions for the cluster; (iii) initially, based on the accuracy estimated for the RXJ1257 cluster ( $\sigma_{\Delta z/1+z} \sim 0.05$  at rest frame, [15]), we defined the cluster photometric redshift range as  $z_{\text{CLUS}} \times (1 \pm \sigma_{\Delta z/(1+z)})$ ; (iv) then we considered as cluster candidates those sources satisfying that 1- $\sigma$  width centred at the central position of the best-fitted Gaussian function to the  $z_{\text{PHOT}}$  distribution is completely included within this cluster photometric redshift range<sup>3</sup>; (v) visual inspection of the best-fitted Gaussian function to the  $z_{\text{PHOT}}$  distribution to eliminate wrong fittings.

### 2.2.1 Photometric redshifts: the LePhare configuration

Using UV/optical/NIR catalogues, we computed the photometric redshifts with the *LePhare* code [9]. *LePhare* computes photometric redshifts based on a  $\chi^2$  SED template-fitting pro-

---

<sup>1</sup>except for the cases of Cl1226 and XMMLSS, where only optical sources were maintained

<sup>2</sup>except for the clusters RXJ1257 and XMMLSS, with 600 and 100 simulations, respectively.

<sup>3</sup>in this step we considered two exceptions: XMMU2235 and XDCP0044. For these two clusters we selected as candidates those sources satisfying that the central position of the best-fitted Gaussian function to the  $z_{\text{PHOT}}$  distribution is included within this cluster range, disregarding its error

cedure. To perform the SED-fitting of the stellar part of the spectrum, we used the BC03 [2] population synthesis models, with star formation histories exponentially declining with time as  $e^{-t/\tau}$ . These type of spectral templates contain the important information about the stellar population of a particular galaxy, so we could determine galaxy properties as the stellar mass, age, metallicity, etc. We included the bands between from UV/optical to IRAC 8  $\mu\text{m}$ . The complete template library was built with the set of BC03 templates included in the *LePhare* repository. These authors considered three different metallicities ( $0.2 Z_{\odot}, 0.4 Z_{\odot}$ , and  $Z_{\odot}$ ) and nine different values of  $\tau$  (up to 30.0 Gyr) with 57 steps in age. In addition, we applied the Calzetti extinction law [3] with ten different values of  $E(B - V)$  (up to 0.9). We assumed the Chabrier IMF [4] and constrained the derived age of each galaxy to be younger than the age of the Universe at the galaxy redshift.

### 2.2.2 Selection of the sample of FIR cluster galaxies

To build the FIR-emitter cluster sample, we cross-matched the full sample of cluster candidates with the MIR/FIR catalogues using the nearest-neighbour technique. Following the methodology of [5], we considered a maximum-error radius of 4'' for the MIPS and PACS catalogues and, since SPIRE photometry was obtained using PACS priors no cross-matching was necessary. Due to the poor accuracy of the criterion which is based only on distance for the FIR counterparts, we made a visual inspection and analysed for each candidate thumbnails of optical/NIR, IRAC 8  $\mu\text{m}$ , MIPS, PACS, and SPIRE bands. In general we discarded sources because of confusion or blending problems or because the match resulted unreliable (the emission clearly corresponds to other source in the field).

## 2.3 SED derived properties

In addition to the position, redshift, and photometry, we derived a set of physical properties for every galaxy in our database. Fixing the redshift to that determined with the Monte Carlo simulations methodology explained above, we execute again the *LePhare* code to determine the stellar mass and the total infrared luminosity, only for the sample of FIR emitters. The database also includes other parameters estimated by *LePhare* as the age of the stellar populations, the extinction, and the UV luminosity. Through the total infrared luminosity we derive the  $SFR_{FIR}$  using the formula from [10], and dividing that by the stellar mass we estimate also the  $sSFR_{FIR}$ .

## 2.4 AGN population and morphology

For all those clusters with the four IRAC bands available, we determine the population of candidates to AGN using the colour-colour diagnostic diagram suggested by [18]. The database includes a flag column indicating whether the galaxy is a candidate to AGN (1), not an AGN (0), or if there is not enough data to perform the classification (-99).

We have performed a morphological classification of cluster galaxies for those clusters at redshift  $\sim$ , by taking advantage of ground-based ( $r'$ -OSIRIS/GTC imaging for RXJ1257) and

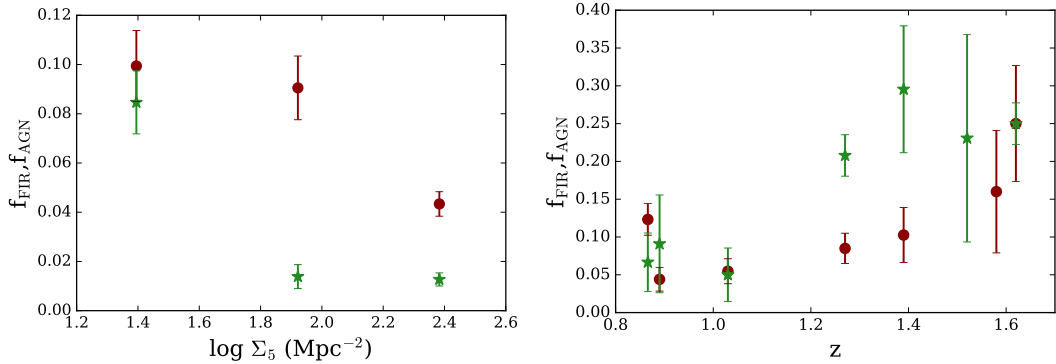


Figure 1: Fraction of the population of FIR emitters, as red circles, and AGN, as green stars, as a function of the local density of galaxies (*left*) and as a function of the redshift (*right*). In left panel error bars were estimated with bootstrapping, varying the limits among the three density environments: low (below the 30th percentile), medium (between percentiles 30 and 70), and high (above the 70th percentile). In the right panel error bars were estimated following Poisson statistics.

space (F814W-WFPC2 and F850LP-ACS/HST for CLJ1226 and WARPSJ1415, respectively) and using non-parametric methods, as implemented in the galSVM code. We were able to classify around the 30 % of the cluster members (the percentage grows up to the 50 % when considering only sources detected in the image used for the classification), obtaining the following numbers of ET/LT galaxies: 22/68, 26/39, and 6/31, for RXJ1257, CLJ1226, and WARPS1415, respectively. A detailed description of the morphological classification of galaxies in the young cluster RXJ1257 could be found in [14]. The database includes the probability of each galaxy to be an early type, with values between 0 (i.e. LT galaxy) and 1 (i.e. ET galaxy).

### 3 Preliminary results

Figures 1 and 2 show preliminary results, and reveal the potential of our database. The large number of photometric cluster galaxies allows us to study the role of the environment as defined by the local galaxy density. We observe in the left panel of Fig. 1 the decrement of the fraction of FIR emitters as a function of the cluster environment: star forming galaxies avoid the densest environments. This behaviour is not always reproduced when analysing individual clusters (see for example [15]). The fraction of AGN seems to be also affected by the environment, showing a steep descent between low and medium densities. The right panel of Fig. 1 shows the evolution of these fractions up to  $z \sim 1.6$ . Although this is still a rough analysis, the plot could suggest the co-evolution of both populations. Figure 2 shows how our sample extends the work of [16] beyond redshift 1. A further analysis must be performed, but we can see how our clusters tend to follow the evolutionary path derived from the low redshift sample.

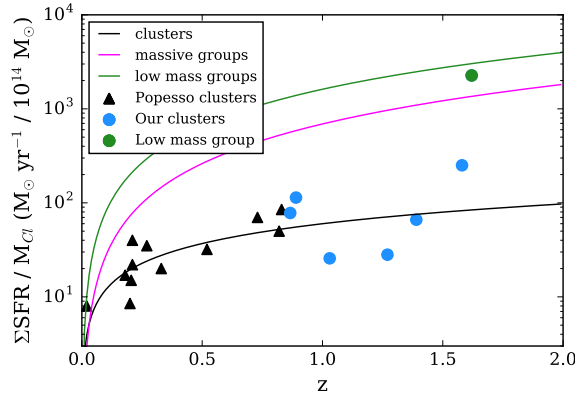


Figure 2: Total SFR per cluster mass as a function of the cluster redshift, considering those cluster galaxies within  $R_{200}$ . Black triangles are clusters from [16], and solid lines are their best fits to clusters (black), massive groups (pink), and low mass groups (green). Blue circles represent our clusters, while the green circle cluster falls within the mass range considered by [16] for the low mass groups.

## References

- [1] Barway, S., Wadadekar, Y., & Kembhavi, A. K. 2011, MNRAS, 410, L18
- [2] Bruzual, G. & Charlot, S. 2003, MNRAS, 344, 1000
- [3] Calzetti, D., Armus, L., Bohlin, R. C., et al. 2000, ApJ, 533, 682
- [4] Chabrier, G. 2003, PASP, 115, 763
- [5] de Ruiter, H. R., Arp, H. C., & Willis, A. G. 1977, A&AS, 28, 211
- [6] Dressler, A. 1980, ApJ, 236, 351
- [7] Geach, J. E., Smail, I., Ellis, R. S., et al. 2006, ApJ, 649, 661
- [8] Gobat, R., Daddi, E., Onodera, M., et al. 2011, A&A, 526, A133
- [9] Ilbert, O., Arnouts, S., McCracken, H. J., et al. 2006, A&A, 457, 841
- [10] Kennicutt, Jr., R. C. 1998, ARA&A, 36, 189
- [11] Li, C. & White, S. D. M. 2010, MNRAS, 407, 515
- [12] Martini, P., Miller, E. D., Brodwin, M., et al. 2013, ApJ, 768, 1
- [13] Martini, P., Sivakoff, G. R., & Mulchaey, J. S. 2009, ApJ, 701, 66
- [14] Pintos-Castro, I., Pović, M., Sánchez-Portal, M., et al. 2016, A&A, 592, A108
- [15] Pintos-Castro, I., Sánchez-Portal, M., Cepa, J., et al. 2013, A&A, 558, A100
- [16] Popesso, P., Biviano, A., Finoguenov, A., et al. 2015, A&A, 579, A132
- [17] Sánchez-Portal, M., Pintos-Castro, I., Pérez-Martínez, R., et al. 2015, A&A, 578, A30
- [18] Stern, D., Eisenhardt, P., Gorjian, V., et al. 2005, ApJ, 631, 163
- [19] Weinmann, S. M., Lisker, T., Guo, Q., Meyer, H. T., & Janz, J. 2011, MNRAS, 416, 1197